Available online at www.sciencedirect.com
SCIENCE DIRECT®
Journal of Power Sources 130 (2004) 42–49
JOURNAL OF POWER SOURCES
www.elsevier.com/locate/jpowsour

Analysis of electrocatalyst degradation in PEMFC caused by cell reversal during fuel starvation

Akira Taniguchi [a], Tomoki Akita [b], Kazuaki Yasuda [b,*], Yoshinori Miyazaki [b]

[a] *The Graduate School of Materials Science, Nara Institute of Science and Technology (NAIST), 8916-5 Takayama, Ikoma, Nara 630-0192, Japan*

[b] *Special Division for Green Life Technology, National Institute of Advanced Industrial Science and Technology, 1-8-31 Midorigaoka, Ikeda, Osaka 563-8577, Japan*

Received 8 December 2003; received in revised form 15 December 2003; accepted 16 December 2003

Abstract

The damage caused by cell reversal during proton exchange membrane fuel cell (PEMFC) operation with fuel starvation was investigated by a single cell experiment. The samples from degraded membrane–electrode assemblies (MEAs) were characterized. Chemical analysis of the anode catalyst layer of MEA samples by energy dispersive X-ray analysis (EDX) clearly showed ruthenium dissolution from the anode catalyst particles. Severe ruthenium loss was observed especially in the fuel outlet region. A reduced carbon monoxide (CO) tolerance was found by CO stripping voltammetry and measurement of deteriorated the fuel cell performance. Surface area loss of the cathode platinum by sintering was also detected by transmission electron microscopy (TEM) analysis and cyclic voltammetry.

Keywords: PEMFC; Fuel cell; Fuel starvation; Cell reversal; Electrocatalyst

1. Introduction

Proton exchange membrane fuel cells (PEMFCs) are promising power sources for electrically powered vehicles and distributed power generation in the near future [1,2]. Small-sized PEMFCs (micro-fuel cells) have also been developed for powering cordless electronic equipment such as laptop computers, cellular phones, power tools, and so on [3].

Reliability and life are the most important considerations in such power sources. However, failure modes for PEM fuel cells are not well documented and degradation causes and mechanisms are not fully understood [4]. There are some factors known to affect the life of PEM fuel cells. The mass transport properties degrade as a result of the accumulation of excess water in the gas diffusion pores [4,5]. Platinum particle sintering in carbon black supported platinum (Pt/C) catalysts can be seen during cell operation [6]. Impurity ions affect the membrane proton conductivity and oxygen reduction kinetics [5,7,8]. In this study, we focus on fuel starvation as a significant problem during PEMFC operation.

It is possible that one or more membrane–electrode assemblies (MEAs) in a stack, or even a complete stack in a multi-stack system, will show a reverse in polarity during fuel cell operation. Various circumstances can result in a fuel cell being driven into voltage reversal by other cells in the series stack. Irreversible damage may be caused to the MEAs by such cell reversal incidents. The most damaging source of cell reversal is reactant starvation, an inadequate supply of fuel, of the MEA at the anode [9]. Fuel and oxidant starvation can occur during a sudden change in reactant demand such as start-up and load change.

There are some reports about a reactant starvation problem in phosphoric acid fuel cell (PAFC) [10–12]. In the early 1990s, Mitsuda and Murahashi studied the changes in the electrode potential in the plane of PAFC under reactant starvation conditions for the Moonlight Project in Japan. This work made it clear that there is a polarization distribution in the horizontal plane of PAFC electrodes by experiment using a single cell equipped with multi-reference electrodes [11,12]. As for the PEMFC, Sanyo Electric reported performance degradation caused by reactant starvation in a national R&D project on PEMFC [13]. There is, however, no literature dealing with the detailed analysis of MEA degradation in a PEMFC under reactant starvation condition. Especially cell reversal can produce severe damage to PEM electrodes and it is necessary to clarify the phenomena occurring in the electrocatalyst. In this study, the characterization of MEAs before and after cell reversal experiment

* Corresponding author. Tel.: +81-727-51-9653; fax: +81-727-51-9629.
E-mail address: k-yasuda@aist.go.jp (K. Yasuda).

0378-7753/$ – see front matter © 2004 Elsevier B.V. All rights reserved.
doi:10.1016/j.jpowsour.2003.12.035

was carried out using high-resolution transmission electron microscopy (TEM), nanosize-energy dispersive X-ray analysis (nano-EDX), X-ray photoelectron spectroscopy (XPS), and electrochemical methods. Especially, this work provides a first attempt of TEM nanostructural characterization and nanochemical analysis of each catalyst particle in the damaged catalyst layer of MEA samples created by the diamond knife ultramicrotomy technique.

2. Experimental

2.1. Preparation of MEA

Electrodes for the PEMFC were prepared from a 40 wt.% carbon black supported platinum electrocatalyst (Johnson Matthey) for the cathode or 30 wt.% Pt/C/15 wt.% Ru/C electrocatalyst (Johnson Matthey) for the anode and a Nafion® solution (5 wt.% solution, E.I. DuPont de Nemours and Company). Catalyst ink was prepared by adding Nafion® solution with isopropyl alcohol to the electrocatalyst powder. The resulting ink was applied on the polytetrafluoroethylene (PTFE) sheet followed by drying and transferred to proton exchange membrane, Nafion® 117 (7 mil thick and 1100 EW sulfonic acid form, DuPont) by hot-pressing in order to manufacture a membrane–electrode assembly. Nafion® content of electrodes were 15 wt.%. The pretreatment of Nafion® membrane was carried out with hydrogen peroxide and 1 mol/l H_2SO_4 aqueous solution. Wet-proofed carbon paper (TGPH 060, Toray) was used as gas diffusion backing.

2.2. Cell reversal experiment

Experiments were carried out in a circular single cell (10 cm^2) made from titanium, the cell A, in order to avoid the effect of cell material corrosion as shown in Fig. 1. The flow field was a conventional parallel channel design [14,15]. This figure also shows the location of the analyzed samples in the cell; location "A" is near the fuel inlet region and "D" and "E" are near the fuel outlet regions. For the cell reversal experiment, fuel (hydrogen gas containing 20% carbon dioxide) and a sufficient amount of oxidant (oxygen) gases were humidified and fed to each electrode. The cell reversal degradation experiment was conducted under the condition of 100% fuel utilization at the current density of 345 mA/cm^2 using the external direct-current power sources. The cell was maintained at 80 °C and the operating pressure was atmospheric. The experimental time was measured from the time when cell terminal voltage reached 0 V.

2.3. Electrochemical characterization

The fuel cell performance was evaluated by measuring the current density against cell voltage (*I–V*) characteristics galvanostatically using the electronic loader (Loaded Impedance Meter SPEC 40026S, Kikusui). For the evaluation of the fuel cell performance, the fuel (pure hydrogen or 50 ppm carbon monoxide (CO) containing hydrogen gas) and oxidant (oxygen) gases were humidified at 80 °C and fed to each electrode at a cell temperature of 80 °C and atmospheric pressure. The *I–V* characteristics were also measured under the condition that humidified pure hydrogen was fed to the anode for evaluation of cathode degradation.

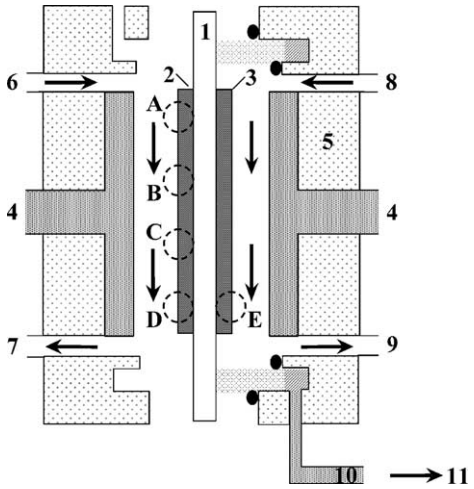

Fig. 1. Schematic drawing of single cell used for the experiment: (1) proton exchange membrane (PEM), Nafion® 117; (2) anode; (3) cathode; (4) current collector; (5) cell housing; (6) fuel inlet; (7) fuel outlet; (8) oxidant inlet; (9) oxidant outlet; (10) liquid junction of 1 M H_2SO_4 aqueous solution when measuring individual electrode potential; (11) reference electrode; and (A–E) location of samples for analysis.

The cyclic voltammograms were taken in situ (in test fuel cell fixtures) on the cathode in order to compare the electrochemically active surface areas. A two-electrode potentiostatic measurement circuit was used for the in situ cyclic voltammetry; hydrated nitrogen was passed through the working electrode (fuel cell cathode) compartment and hydrated hydrogen went through the counter electrode (fuel cell anode) compartment. The profiles were recorded at a scan rate of 50 mV/s using an electrochemical analyzer (BAS100B/W).

CO stripping voltammetry on the MEA anode was performed. Following sufficient purging of the cathode compartment with nitrogen, hydrogen gas was passed through the cathode which was used as both the counter electrode and reference electrode. The anode was held at the adsorption potential, 150 mV versus the counter electrode (RHE), and 1000 ppm CO in hydrogen gas was passed through the anode. After CO adsorption for 20 min, the bulk CO was removed by feeding pure nitrogen through it. Stripping voltammograms were collected between 150 mV (starting potential) and 850 mV at a scan rate of 30 mV/s at room temperature. Complete oxidation of the adsorbed species was accomplished in a single scan; no oxidation was monitored during the second scan.

For measurement of the behavior of the individual electrode potentials during the cell reversal experiment, the cell

connected to a standard hydrogen electrode by a H_2SO_4 electrolyte junction was used as shown in Fig. 1. For this experiment, the cell housing made from PTFE, the cell B, was used. The current collectors were made from titanium. The periphery of the electrode was filled with 1 M H_2SO_4 aqueous solution. A Viton® gasket is located between electrode and H_2SO_4 aqueous solution. The standard hydrogen electrode was connected to the membrane at the periphery of the electrode by 1 M H_2SO_4 aqueous solution as shown in our previous paper [16].

2.4. Characterization by TEM, EDX, and XPS

A small piece was removed from the MEA for preparation of the TEM sample and carbon paper was peeled from both plane of this piece. The cross-section of the MEA sample was prepared via epoxy impregnation and ultramicrotome sectioning using a diamond knife. Samples for the TEM observations were directly supported on a copper mesh with a carbon micro-grid. The TEM observation was performed using a JEOL JEM-3000F electron microscope at an accelerating voltage of 300 kV. The particle size distribution measurements were performed on digital images using the image analyzing software Image-Pro. The TEM was equipped with a nano-EDX device for analysis of the elemental composition in the nanosize region.

A small piece of a MEA sample was also characterized on a larger scale using a field emission scanning electron microscope (SEM, JSM-6700FA, Jeol) equipped with EDX (EX-2300BU, Jeol) for elemental analysis of the MEAs.

For the XPS measurements, a small piece removed from the MEA and carbon paper on both sides was placed on the sample holder. XPS measurements of the catalyst layer were performed using a SHIMADZU ESCA-3400. Since reproducible separation of the catalyst layer from the membrane after hot-pressing is very difficult, the XPS was measured on the back surface of the catalyst layer after separation of the carbon paper.

3. Results and discussion

Cell reversal occurs when the fuel cell stack is loaded and not enough fuel is supplied to the anode. Drawing excessive current from any one cell—more than its fuel delivery can produce—can lead to cell reversal. In this study, an experiment using a single cell that mimics the cell reversal in a stack was carried out. After the cell reversal degradation experiment under the condition of 100% fuel utilization using external direct-current power sources, various characterizations was carried out.

The potential change of the cell terminal voltage and individual electrodes during the cell reversal experiment was measured using the cell B connected to a reference electrode by an electrolyte junction. The typical time-dependent change of the cell terminal voltage during an experiment is shown in Fig. 2. In addition, this figure shows the time-dependent change of the anode and cathode potentials versus RHE. It was observed that the cell terminal voltage rapidly dropped to the negative voltage and the MEA changes polarity due to cell reversal as soon as the experiment started. After this initial rapid drop, the cell terminal voltage showed a steady decrease with time. Cell reversal occurred when the anode potential increased and became more positive than the cathode potential. The anode potential quickly increased to near 1.5 V. This result indicates that the anode potential increased until water electrolysis occurs as soon as the experiment started since the anode was starved of fuel [9].

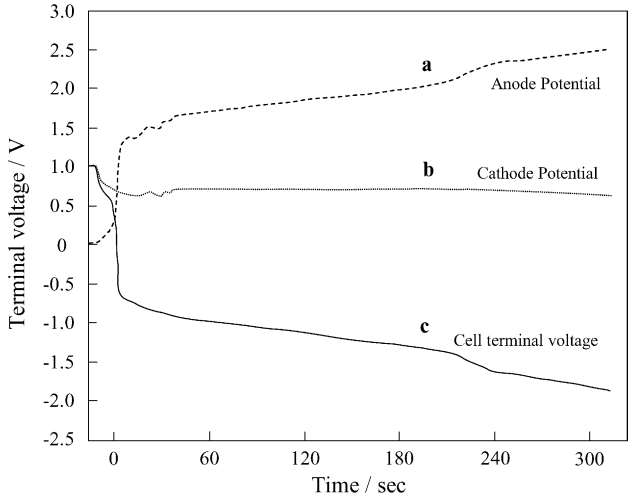

Fig. 2. The time-dependent changes of the anode and cathode potential during the cell reversal experiment.

Fig. 3 shows *I–V* curves of the cell after different experimental periods during the cell reversal test using the cell A. These curves were measured under the condition where enough hydrogen fuel containing 50 ppm CO was supplied. The original performance of the cell was lowered by increasing the experimental time. Especially, the performance of

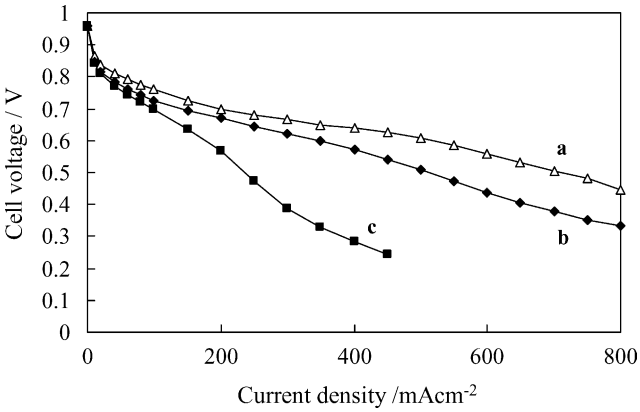

Fig. 3. The change in current–voltage performance of PEMFC by cell reversal experiment: (a) before experiment; (b) after experiment for 3 min; and (c) after experiment for 7 min.

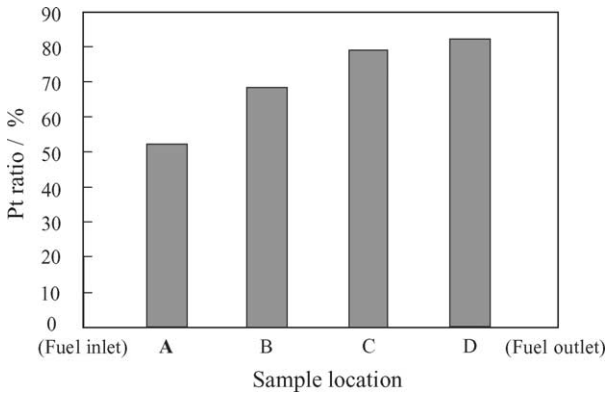

Fig. 4. The dependence of the Pt ratio to Ru, Pt/(Ru + Pt), of the anode catalyst layer after the cell reversal experiment for 2 min determined by EDX on the sample location.

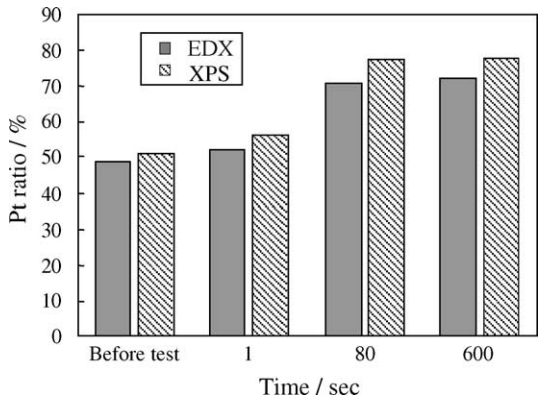

Fig. 5. The relative changes in the Pt ratio to Ru, Pt/(Ru + Pt), near the fuel outlet region before and after the cell reversal experiment at different times determined by EDX and XPS.

the cell after cell reversal for 7 min showed the typical form of anode CO poisoning [17]. This kind of degradation behavior suggests deterioration of CO tolerance by the anode catalyst.

The carbon black supported platinum–ruthenium alloy catalyst (PtRu/C) is the state of the art anode catalyst for a reformed fuel gas mixture containing a small amount of carbon monoxide, a severe poison for Pt. The cross-section of the MEA was characterized by EDX attached to the SEM for determining the molar composition of the noble metals in the anode catalyst layer. The relative changes in the Pt:Ru ratio before and after the cell reversal experiment provided information to assess the anode catalyst degradation. The change in the Pt:Ru ratio, Pt/(Ru + Pt), of the PEMFC anode plane under cell reversal for 2 min is shown in Fig. 4. A significant decrease in the Ru content was detected in the region located near the fuel outlet area. The platinum ratio increased in the direction from the fuel inlet region to the fuel outlet region as shown in this figure. In the anode of the PEM fuel cells operated on reformed gas for practical use, the hydrogen concentration downstream is significantly reduced compared with that upstream. This change indicates that the region where fuel starvation occurs severely suffer from degradation in the the anode plane.

Fig. 5 shows the relative changes in the Pt:Ru ratio, Pt/(Ru + Pt), near the fuel outlet region before and after the cell reversal experiment at different times. It was observed that the platinum ratio of the anode catalyst layer clearly increased after cell reversal. The Pt:Ru ratio of the anode catalyst layer was also measured using the XPS as shown in this figure. Strictly speaking, the XPS measurement might not reflect the status of the interface between the catalyst layer and membrane, which is the most important electrochemical reaction zone [18], because of measurement on the back surface of the catalyst layer. However, the results were similar to those measured by EDX. The values for degraded samples measured by XPS were slightly higher than those by EDX. Although nearly bulk information about the catalytic active particles can be obtained by XPS since the particle size is very small, the higher Pt ratio measured by XPS possibly suggests a Pt surface rich composition of catalyst particles.

A typical TEM micrographic image of the anode catalyst layer sample after the cell reversal experiment for 10 min is shown in Fig. 6. The terminal voltage reached about −1.2 V at 10 min. This TEM micrograph was recorded in the dark field mode. The TEM image shows catalytic active particles distributed on the surface of the carbon black support. The best technique to determine the molar composition of noble metals in individual catalyst particles is high-resolution TEM combined with nano-EDX. On-particle nano-EDX analysis was performed to identify the Ru present in the individual catalyst particles. Fig. 7 shows platinum ratios of individual catalyst particles in the fuel outlet region

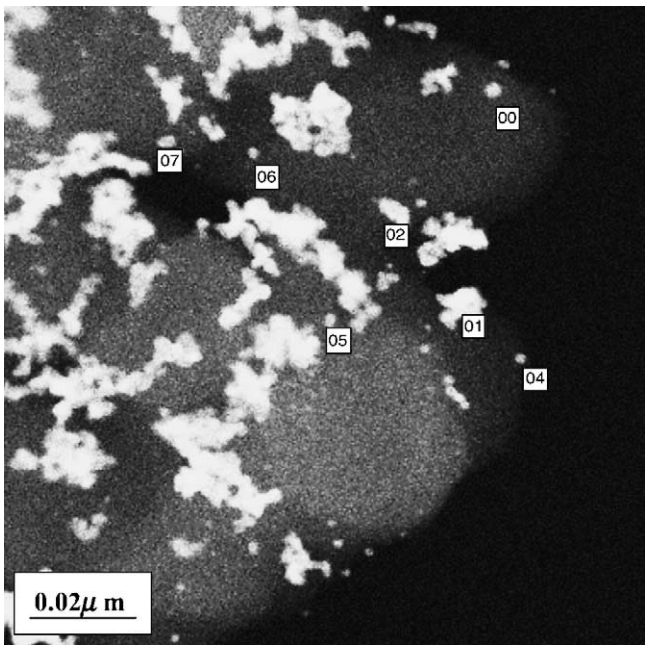

Fig. 6. A typical TEM micrographic image of the anode catalyst layer sample after the cell reversal experiment for 10 min.

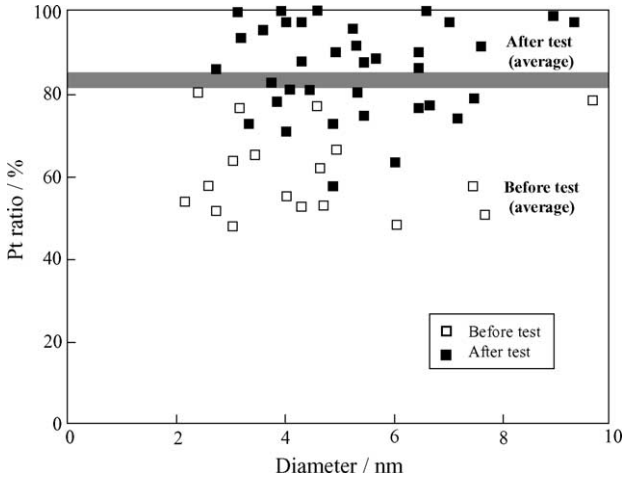

Fig. 7. The platinum ratios of individual catalyst particles in the fuel outlet region before and after the degradation experiment for 10 min evaluated from the on-particle EDX.

before and after the degradation experiment for 10 min evaluated from the on-particle EDX spectra. “Average” means the value determined by EDX analysis in the order of a few micrometers. The tendency of Pt-rich composition in smaller particles can be seen for the catalyst before experiment. This figure clearly shows that the Ru concentration of individual particles decreased by cell reversal experiment. Even particles containing no ruthenium were found. Ruthenium was detected in neither the membrane nor the cathode side. However, a small amount was detected with platinum in the anode carbon paper. From these facts, ruthenium was considered to be dissolved away during the cell reversal experiment. Fig. 8a and b demonstrate the particle size distribution for the anode catalyst before and after the degradation experiment for 10 min as determined from the high-resolution TEM images. The particle size distribution of the catalyst particle after the experiment became broader than that before the experiment. The average particle size increased from 2.64 to 4.95 nm. From these facts, Pt is also considered to be dissolved and reprecipitated during cell reversal. The corrosion of the carbon support was not able to be distinguished from this high-resolution TEM observation.

In situ CO stripping voltammetry of the MEA anode was performed for evaluation of the anodic oxidation ability for adsorbed CO on platinum. Fig. 9 shows the time-dependent change of the peak potential for adsorbed CO oxidation of the degraded MEA anode determined from the CO stripping voltammetry using cathode fed with hydrogen as the RHE. The position of the potential corresponding to the maximum CO stripping current density significantly depends on the period of the cell reversal experiment. In the case of pure platinum, the adsorbed CO layer was oxidized at a current peak with a maximum at 640 mV versus RHE. The maximum CO stripping peak position shifted from the initial value of 378 mV in the positive direction with time toward that of the electrode made of a pure platinum electrocatalyst.

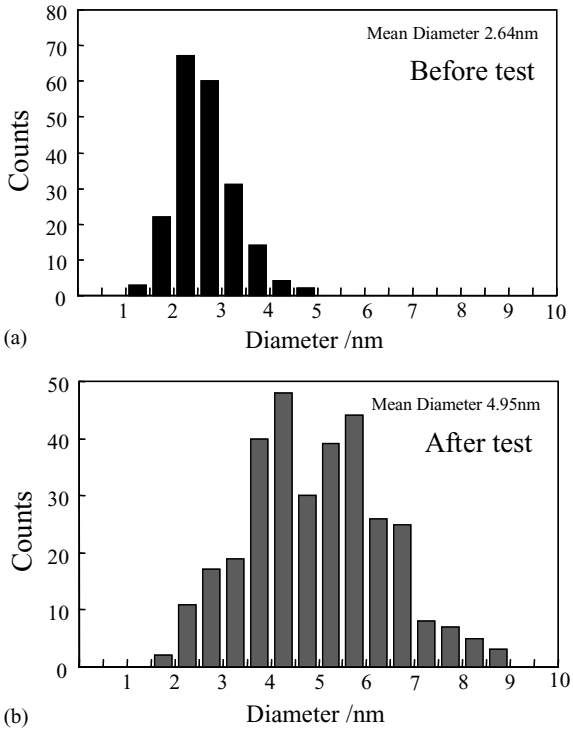

Fig. 8. The distribution of the particle size for the anode catalyst: (a) before and (b) after the degradation experiment for 10 min determined from high-resolution TEM images.

This figure clearly shows that the adsorbed CO oxidation activity was reduced by dissolution of the ruthenium in the catalyst particles. As shown in Fig. 2, the anode potential increased as soon as the experiment started since the anode was starved of fuel. It is known that the standard potential of the Ru/Ru^{2+} couple is 0.46 V [25]. Therefore, Ru dissolution in the anode is considered to occur because of this high anode potential. As the anode potential increases gradually with time, platinum dissolution–redeposition also becomes easier to occur.

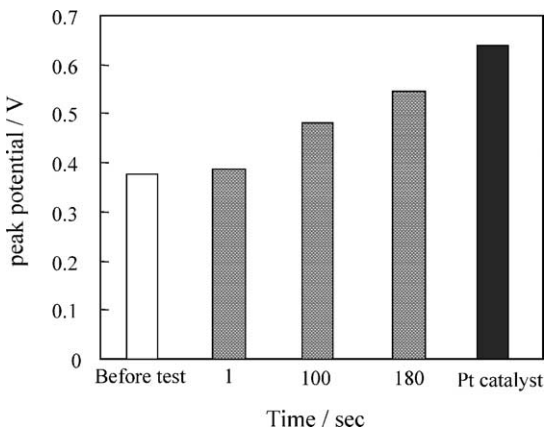

Fig. 9. Experimental time-dependent change of peak potential for adsorbed CO oxidation of degraded MEA anode determined from the CO stripping voltammetry.

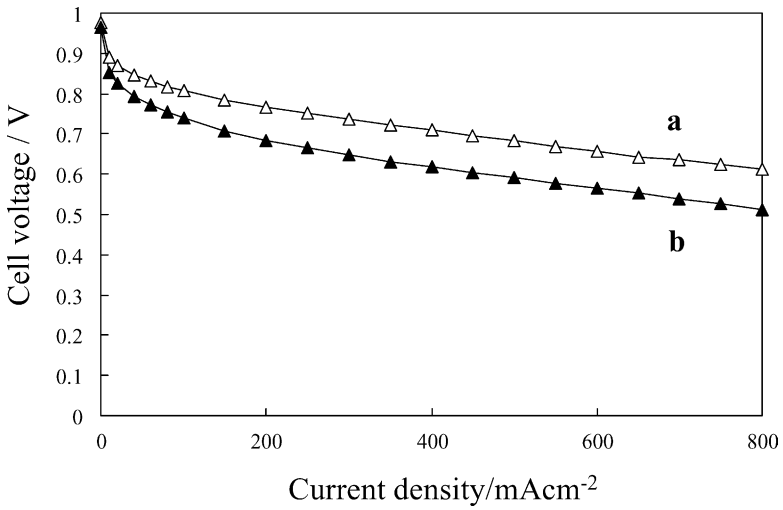

Fig. 10. Comparison of *I–V* characteristics of the cell before and after the cell reversal experiment for 10 min under the condition of a pure hydrogen supply as the fuel.

Now the effect on the cathode is considered. Fig. 10 shows *I–V* curves of before and after the cell reversal experiment for 10 min. These curves were measured under the condition where enough pure hydrogen fuel was supplied. There can be seen a performance loss due to the cell reversal. In the case of pure hydrogen fuel, the anode overpotential can be usually almost negligible without regard to Pt or PtRu as the anode catalyst [19]. Therefore, this degradation may be attributed to cathode degradation.

The in situ cyclic voltammetry is useful in assessing the electrochemically active surface area of the MEA catalyst layer [20,21]. This method was performed for comparing the electrochemically active surface area of the fuel cell cathodes. Fig. 11 shows the cyclic voltammograms before and after the cell reversal experiments. The effect of the cell reversal on the hydrogen adsorption and desorption features is shown in this figure. The hydrogen adsorption and desorption area, the electrochemically active surface area of the cathode, decreased during the cell reversal experiments. It was initially assured that the process of the cyclic voltammetry measurement itself was not contributing to the hydrogen adsorption and desorption features. Therefore, these facts mean that the electrochemically active surface area decreased with the period of the cell reversal experiment and by approximately 28% in 3 min of cell reversal. A similar degradation phenomenon at the cathode caused by anode fuel shortage was reported by Sanyo although details of experiment were not clear [13]. It should be noticed that degradation appeared on the electrochemical surface area after only 1 s of operation under cell reversal conditions as shown in this figure.

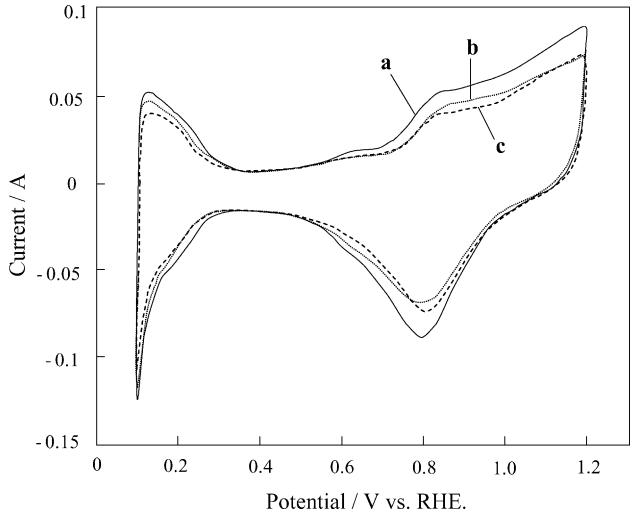

Fig. 11. Comparison of cyclic voltammograms for cathode: (a) before test; (b) after test for 1 s; and (c) after test for 3 min.

A TEM analysis was performed on the cathode catalyst layer of the MEA. Fig. 12a and b show TEM images of the sample before and after the cell reversal experiment for 10 min. Fig. 13a and b show the particle size distribution of for cathode catalyst determined from the TEM images. The average particle size increased from 2.81 to 4.04 nm. In the sample before the experiment, the smallest detected particles have a size of 1.0–1.5 nm as can be seen in the image (Fig. 12a) and the particle size distribution (Fig. 13a). However, these smallest particles disappeared in the image of the sample after the cell reversal experiment (Figs. 12b and 13b). The loss of platinum surface area through sintering or recrystallization within the porous cathode has been proposed to be the principal reason for the decline of activity in phosphoric acid fuel cells [22–24]. Such catalyst degradation can occur through the surface migration of platinum and platinum dissolution–redeposition with the driving force being the high free energy of the small platinum particles. The decrease in the electrochemically active surface area can be linked to an increase in the platinum particle size. As shown in Fig. 2, the change in the cell terminal voltage

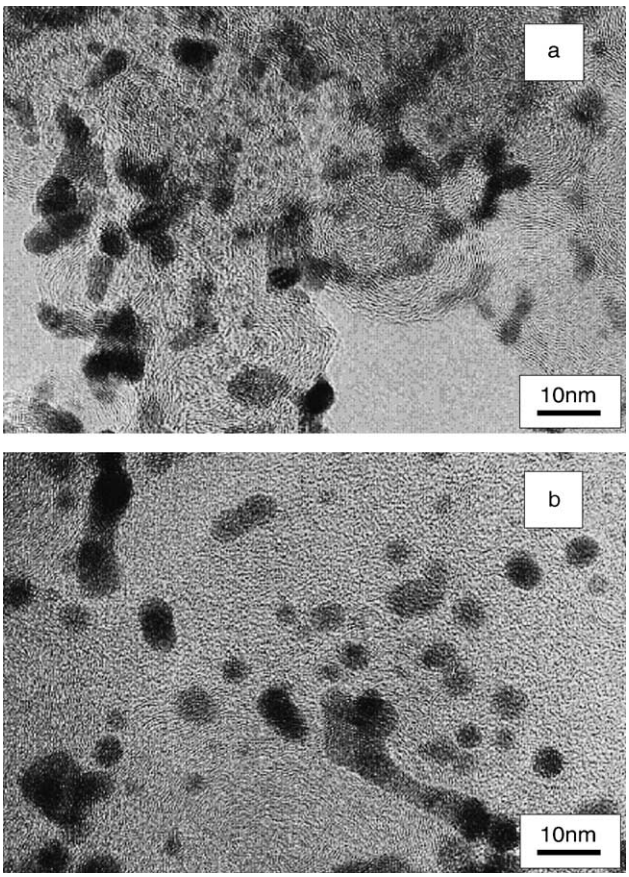

Fig. 12. TEM images of the cathode catalyst before and after the cell reversal experiment for 10 min.

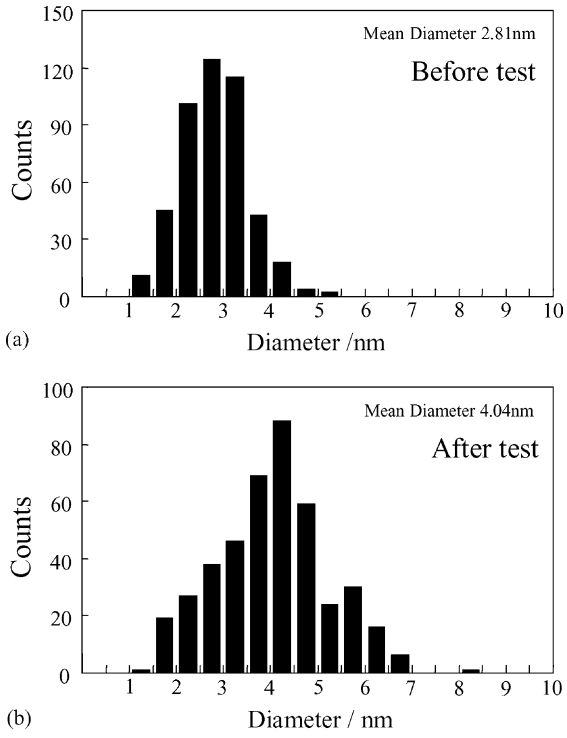

Fig. 13. The particle size distribution for cathode catalyst: (a) before and (b) after degradation experiment for 10 min determined from TEM images.

reflects the anode potential. The cathode potential was stable near 0.7 V during the experiment. Therefore, the cathode degradation by cell reversal cannot be explained from these measurements.

Although the severe phenomena caused by cell reversal were clarified in these experiments, there remain unknown reasons for the unchanged Pt ratio at the inlet area in spite of such a high anode potential and for the degradation of the cathode in spite of the usual cathode potential. Mitsuda and Murahashi [11,12] reported a significant potential shift occurs in the positive direction in the fuel outlet area of the anode using the cell furnished with a multi-reference electrode. Since the electrode potential measured in our experiment is considered to indicate the average value of the electrode plane, it is necessary to electrochemically study the potential distribution in the anode plane by developing analysis technology suitable for PEMFC in the next investigation. Cell reversal caused by fuel starvation results in the production of oxygen instead of hydrogen oxidation at the anode through the oxidation of water. Therefore, other than an electrochemical reason, it is possible that generated oxygen might cause a local heat generation, which results in the anode catalyst degradation and also affects cathode degradation. The fact that the operation using a thinner membrane, Nafion® 112 (2 mil thick), easily resulted in membrane breakthrough suggests the effect of local heat generation. These points are the subjects of a subsequent publication.

4. Conclusion

Degradation phenomena in electrocatalyst caused by cell reversal during the operation under the condition of fuel starvation were characterized using TEM, EDX, and electrochemical methods. It was found that ruthenium dissolution from individual catalyst particles occurred in the anode catalyst layer. There were distributions in the Ru dissolution in the anode plane and the area closer to the outlet region that suffered from severer degradation. The surface area loss of the cathode platinum particle by cell reversal was also detected. The behaviors of both electrodes were measured and anode degradation could be attributed to the high anode potential. Fuel starvation caused severe and permanent damage to the electrocatalyst of the PEMFC and it must be absolutely avoided even if the operation under fuel starvation is momentary.

Acknowledgements

This work was financially supported by the New Energy and Industrial Technology Development Organization (NEDO) as a part of the research and development of polymer electrolyte fuel cell technology project directed by the Ministry of Economy, Trade and Industry (METI). The authors thank T. Ioroi and T. Tanaka for their contributions to

this work. The authors are grateful to M. Hayashi for work on the size distribution measurements of the catalyst particles and also to K. Yagi for his help in the experimental work. T. Fuyuki, professor of NAIST, is gratefully acknowledged for the helpful discussions and support.

References

[1] P. Costamagna, S. Srinivasan, J. Power Sources 102 (2001) 253.
[2] F. Preli, Fuel Cells 2 (2002) 5.
[3] C.K. Dyer, J. Power Sources 106 (2002) 31.
[4] M. Fowler, R.F. Mann, J.C. Amphlett, B.A. Peppley, P.R. Roberge, in: W. Vielstich, H.A. Gasteiger, A. Lamm (Eds.), Handbook of Fuel Cells—Fundamentals, Technology and Applications, vol. 3, Fuel Cell Technology and Applications, Wiley, 2003, pp. 663.
[5] J. St-Pierre, D.P. Wilkinson, S. Knights, M.L. Bos, J. New Mater. Electrochem. Syst. 3 (2000) 99.
[6] M.S. Wilson, F.H. Garzon, K.E. Sickafus, S. Gottesfeld, J. Electrochem. Soc. 140 (1993) 2872.
[7] L. Ma, S. Warthesen, D.A. Shores, J. New Mater. Electrochem. Syst. 3 (2000) 221.
[8] T. Okada, Y. Ayato, H. Satou, M. Yuasa, I. Sekine, J. Phys. Chem. B 105 (2001) 6980.
[9] T.R. Ralph, M.P. Hogarth, Platinum Met. Rev. 46 (2002) 117.
[10] Y. Tsutsumi, I. Sone, Y. Nanba, in: Abstract of the 1986 Fuel Cell Seminar, 1986, p. 110.
[11] K. Mitsuda, T. Murahashi, J. Appl. Electrochem. 21 (1991) 524.
[12] K. Mitsuda, T. Murahashi, J. Electrochem. Soc. 137 (1990) 3079.
[13] S. Sakamoto, M. Karakane, H. Maeda, Y. Miyake, T. Susai, T. Isono, in: Abstract of the 2000 Fuel Cell Seminar, 2000, p. 141.
[14] K. Scott, W.M. Taama, P. Argyropoulos, J. Appl. Electrochem. 28 (1998) 1389.
[15] V. Nguyen, J. Electrochem. Soc. 143 (1996) L103.
[16] M. Mizuhata, K. Yasuda, K. Oguro, H. Takenaka, Denki Kagaku 64 (1996) 692.
[17] R.A. Lemons, J. Power Sources 29 (1990) 251.
[18] D. Bevers, M. Wohr, K. Yasuda, K. Oguro, J. Appl. Electrochem. 27 (1997) 1254.
[19] D. Bernadi, M. Verbrugge, J. Electrochem. Soc. 139 (1992) 2477.
[20] O.J. Murphy, G. Duncan, D.J. Manko, J. Power Sources 47 (1994) 353.
[21] H. Kumpulainen, T. Peltonen, U. Koponen, M.B. Ergelin, M. Valkiainen, M. Wasberg, VTT Tiedotteita 2137 (2002) 1.
[22] P. Bindra, S.J. Clouser, E. Yeager, J. Electrochem. Soc. (1979) 1631.
[23] P. Stonehart, P.A. Zucks, Electrochim. Acta 17 (1972) 2333.
[24] J.A. Bett, K. Kinoshita, P. Stonehart, J. Catal. 35 (1974) 307.
[25] R. Woods, in: J. Bard (Ed.), Electroanalytical Chemistry, vol. 9, M. Dekker, 1976, p. 11.